

See discussions, stats, and author profiles for this publication at: <https://www.researchgate.net/publication/223991234>

Influence of Charge on Anion Receptivity in Amide-Based Macrocycles

ARTICLE in INORGANIC CHEMISTRY · MARCH 2012

Impact Factor: 4.76 · DOI: 10.1021/ic300260g · Source: PubMed

CITATIONS

8

READS

29

5 AUTHORS, INCLUDING:



Md. Alamgir Hossain

Bangladesh Agricultural University

69 PUBLICATIONS 1,384 CITATIONS

SEE PROFILE



Sung Ok Kang

47 PUBLICATIONS 1,744 CITATIONS

SEE PROFILE



Victor W Day

University of Kansas

295 PUBLICATIONS 9,030 CITATIONS

SEE PROFILE



Kristin Bowman-James

University of Kansas

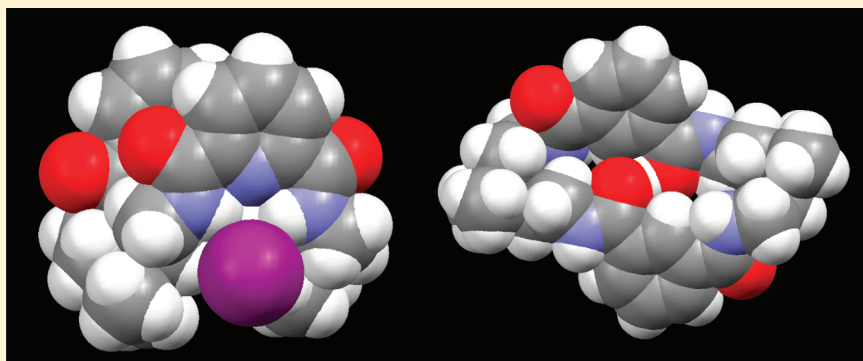
88 PUBLICATIONS 3,650 CITATIONS

SEE PROFILE

Influence of Charge on Anion Receptivity in Amide-Based Macrocycles

Md. Alamgir Hossain,[†] Sung Ok Kang,[‡] Jerry Alan Kut,[‡] Victor W. Day,[‡] and Kristin Bowman-James^{*‡}[†]Department of Chemistry and Biochemistry, Jackson State University, 1400 J. R. Lynch Street, Jackson, Mississippi 39217, United States[‡]Department of Chemistry, University of Kansas, Lawrence, Kansas 66045, United States

S Supporting Information



ABSTRACT: Binding and structural aspects of anions with tetraamido/diquaternized diamino macrocyclic receptors containing *m*-xylyl, pyridine, and thiophene spacers are reported. ¹H NMR studies indicate that the quaternized receptors display higher affinities for anions compared to corresponding neutral macrocycles. The macrocycles containing pyridine spacers consistently display higher affinity for a given anion compared to those with either *m*-xylyl or thiophene spacers. The *m*-xylyl- and pyridine-containing receptors exhibit high selectivity for H₂PO₄[−] in DMSO-*d*₆ with association constants, *K*_a = 1.09 × 10⁴ and >10⁵ M^{−1}, respectively, and moderate selectivity for Cl[−] with *K*_a = 1.70 × 10³ and 5.62 × 10⁴ M^{−1}, respectively. Crystallographic studies for the Cl[−] and HSO₄[−] complexes indicate that the *m*-xylyl-containing ligand is relatively elliptical in shape, with the two charges at ends of the major axis of the ellipse. The anions are hydrogen bonded with the macrocycle but are outside the ligand cavity. In the solid state, an unusual low-barrier hydrogen bond (LBHB) was discovered between two of the macrocycle's carbonyl oxygen atoms in the HSO₄[−] complex. The pyridine-containing macrocycle folds so that the two pyridine units are face-to-face. The two I[−] ions are chelated to the two amides adjacent to a given pyridine. In the structure of the thiophene containing macrocycle with two BPh₄[−] counterions, virtually no interaction was observed crystallographically between the macrocycle and the bulky anions.

■ INTRODUCTION

Anions play key chemical roles both in living systems and in the environment. It is not surprising, therefore, that considerable research is being focused on understanding the basic relationships of anion binding through the design and synthesis of receptors capable of selective binding for target anions.^{1–3} Although the field began with a focus on polyammonium hosts, it has now expanded to amides and thioamides, ureas and thioureas, and a number of other hydrogen bond donor groups including, but not limited to, carbazoles, indoles, biindoles, indolocarbazole, and pyridinium hosts. In nature, however, amides in proteins are key binding entities for anions, for example, in the sulfate and phosphate binding proteins.⁴ As such, our research has focused recently on amide- and related thioamide-based receptors^{5–7} with an interest in potential applications in anion extraction, especially as related to nuclear waste remediation.⁸ However, during the course of the current study, the rather unusual occurrence of a very short intramolecular

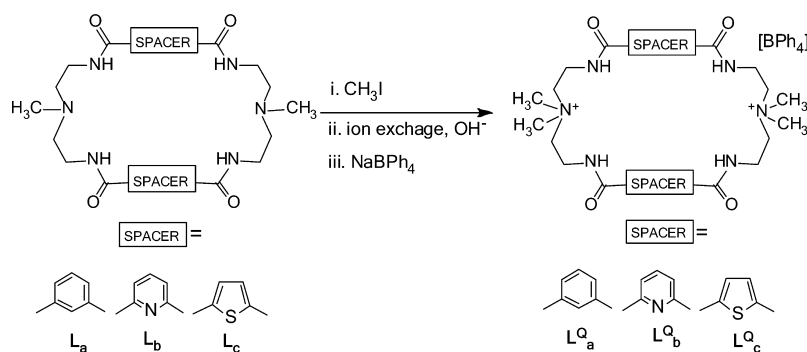
interaction between the two carbonyl oxygen atoms in the HSO₄[−] complex, provided an interesting new slant on the potential significance of these structures.⁹

During our survey of mixed amide/amine hosts, **L**, we observed that the presence of the tertiary amine groups seemed to play a role in enhancing the selectivity and binding of tetraamide-based receptors for the oxo acids, HSO₄[−] and H₂PO₄[−].⁵ We attributed these findings to a dual receptivity of the host: the amide Lewis acid affinity for the anion's oxygen atoms as well as the Lewis base affinity of the amines for the oxo acid protons. This then led to the next generation of receptors, designed to contain a stable dipositive charge in the absence of amine NH protons, by quaternization of two tertiary amines, **L**^{Q2+} (Scheme 1).¹⁰

There have been other reports of dual receptors, binding via both hydrogen bonds and charge. For example, Beer, Drew, and

Received: February 3, 2012

Published: March 30, 2012

Scheme 1. Synthetic Pathway of Mixed Amide/Quaternary Amine Macrocycles, L_{a-c}^{Q-2+} 

co-workers reported an amide-based *cleft* with a pyridinium group that was used to form a pseudorotaxane.¹¹ Expectations were that the acidity of the NH proton would be increased due to the presence of positive charge. Schmidtchen and co-workers reported porphyrins with appended secondary amide and quaternary amine groups, which were used for the binding of saccharides.¹² However, the mixed amide/quaternized amine macrocycles reported herein represent a different dual donor class of anionophores incorporating both hydrogen bonding and non-hydrogen bonding electrostatic forces within a single macrocyclic framework. In the case of dinegative anions, the presence of the two positive centers serves to provide consistent charge complementarity, thus eliminating the need for external cations.

One of the unanticipated findings of this study was of an unusually short *intramolecular* hydrogen bond. *Intermolecular* hydrogen bonds involving hemiprotonated amide oxygen atoms have been the subject of a number of reports.¹³ Bruce and co-workers reported a short *intramolecular* hydrogen bond involving a carbonyl and hydroxyl group in benzoylacetone.¹⁴ However, examples of short *intramolecular* amide carbonyl $O\cdots H^+\cdots O$ bonds are rare.¹⁵ Bonds that are extremely short, such as that observed in the HSO_4^- complex reported here and previously communicated⁹ are not common and are known as low-barrier hydrogen bonds (LBHB).¹⁶

In this Article, we report the synthesis of macrocyclic receptors L_{a-c}^{Q-2+} incorporating amide and quaternized amine groups with different spacers, as well as the results of NMR binding studies for a series of anions in DMSO- d_6 . Crystallographic findings of the Cl^- complex and the LBHB in the HSO_4^- complex with L_a^{Q-2+} , of the I^- complex with L_b^{Q-2+} , and the BPh_4^- salt of L_c^{Q-2+} are also described.

EXPERIMENTAL SECTION

General. [n -Bu₄N]⁺A[−] (A[−] = H₂PO₄[−], HSO₄[−], NO₃[−], Cl[−], Br[−], I[−], and ClO₄[−]) were purchased from Aldrich. Other chemicals were reagent grade and were used without further purification. All samples were thoroughly dried under vacuum at 60 °C for 24 h prior to the binding studies. Nuclear magnetic resonance (NMR) spectra were recorded on a Bruker AM 500 spectrometer at 500 MHz. Chemical shifts of the protons are expressed in ppm and calibrated against TMS as an external reference. Elemental analyses were performed at Desert Analytics, Tucson, AZ. Mass spectral data were obtained from the Mass Spectrometry Laboratory at the University of Kansas on a ZAB HS Mass spectrometer.

Synthesis. L_{a-b} . The neutral receptors, L_a and L_b , were synthesized from the reaction of *N*-methyl-2,2'-diaminodiethylamine and the corresponding diacid chloride under high dilution in CH₂Cl₂, as reported previously.^{5,6}

L_c . The thiophene containing macrocycle, L_c , was synthesized from the reaction of *N*-methyl-2,2'-diaminodiethylamine and 2,5-thiophenedicarbonyl dichloride following the same method as that for L_a and L_b . Yield: 12%. ¹H NMR (500 MHz, DMSO- d_6 , TMS): δ 2.20 (s, 6H, CH₃), 3.18 (d, 8H, NCH₂), 3.37 (d, 8H, NCH₂), 7.38 (s, 4H, ArH), 7.99 (t, 4H, NH). FAB MS: m/z 507.2 [M+1]⁺. Anal. Calcd for C₂₂H₃₀N₆O₄S₂·HCON(CH₃)₂: C, 51.79; H, 6.43; N, 16.91. Found: C, 51.05; H, 6.62; N, 16.70.

$L_{a-c}^{Q-2+} \cdot 2I^-$. The neutral amide L_{a-c} (0.22 mmol) was dissolved in CH₃CN/CH₃OH (5:2 v/v, 5 mL), and an excess amount of CH₃I (0.80 mmol) was added to the solution. The resulting mixture was stirred for 3 days at room temperature. The iodide salt precipitated as a white solid and was separated by filtration.¹⁰ The product was washed with CH₃OH and dried in vacuo.

$L_a^{Q-2+} \cdot 2I^-$. Yield 80%. ¹H NMR (500 MHz, DMSO- d_6): δ 3.22 (s, 12H, CH₃), 3.62 (t, 8H, NCH₂), 3.72 (m, 8H, NCH₂CH₂), 7.50 (t, 2H, ArH3), 7.90 (d, 4H, ArH2), 8.23 (s, 2H, ArH), 8.92 (b, 4H, NH). FAB MS: m/z 652 [M − I]⁺, 523 [M − HI₂]⁺. Anal. Calcd for C₂₈H₄₀N₆O₄I₂: C, 43.18; H, 5.18; N, 10.79. Found: C, 42.94; H, 5.08; N, 10.68.

$L_b^{Q-2+} \cdot 2I^-$. Yield 70%. ¹H NMR (500 MHz, DMSO- d_6) δ 3.25 (s, 12H, CH₃), 3.72 (t, 8H, NCH₂), 3.83 (m, 8H, NCH₂CH₂), 8.12 (m, 6H, ArH), 9.38 (b, 4H, NH). FAB MS m/z 653 ([M − I]⁺, 525 ([M − HI₂]⁺. Anal. Calcd for C₂₆H₃₈I₂N₆O₄·1.5H₂O: C, 38.66; H, 5.12; N, 13.88. Found: C, 38.86; H, 5.10; N, 13.66.

$L_c^{Q-2+} \cdot 2I^-$. ¹H NMR (500 MHz, DMSO- d_6) δ 3.21 (s, 12H, CH₃), 3.55 (t, 8H, NCH₂), 3.66 (t, 8H, NCH₂CH₂), 7.44 (d, 4H, ArH), 8.69 (t, 4H, NH). Yield 70%. FAB MS m/z 663 ([M − I]⁺, 535 ([M − HI₂]⁺. Anal. Calcd for C₂₄H₃₆I₂N₆O₄S₂·1.5H₂O: C, 35.25; H, 4.80; N, 10.27. Found: C, 35.08; H, 4.71; N, 10.04.

$L_{a-c}^{Q-2+} \cdot 2BPh_4^-$. The iodide salt $L_{a-c}^{Q-2+} \cdot 2I^-$ (0.12 mmol) was suspended in a mixture of H₂O and CH₃OH (1:1 v/v, 5 mL). A few drops of DMSO were added to obtain a clear solution. The solution was passed through an ion-exchange column (Dowex, 1 × 8–200, OH[−]) to form $L_{a-c}^{Q-2+} \cdot 2OH^-$. The basic solution (as monitored by pH paper) was collected, and the solvent was evaporated to give a white solid. The product was redissolved in a mixture of H₂O and CH₃OH (1:1 v/v, 2 mL), and a solution of NaBPh₄ (0.26 mmol) in CH₃OH (2 mL) was added slowly to form $L_{a-c}^{Q-2+} \cdot 2BPh_4^-$ as a white powder. The solid was filtered and washed with H₂O and CH₃OH and dried in vacuo.

$L_a^{Q-2+} \cdot 2BPh_4^-$. Yield 85%. ¹H NMR (500 MHz, DMSO- d_6): δ 3.20 (s, 12H, CH₃), 3.63 (t, 8H, NCH₂), 3.72 (m, 8H, NCH₂CH₂), 6.79 (t, 8H, BArH), 6.92 (t, 16H, BArH), 7.17 (d, 16H, BArH), 7.49 (t, 2H, ArH3), 7.90 (d, 4H, ArH2), 8.22 (s, 2H, ArH), 8.92 (b, 4H, NH). FAB MS: m/z 843 [M − BPh₄]⁺, 532 [M − H(BPh₄)₂]⁺. Anal. Calcd for C₇₆H₈₀N₆O₄B₂: C, 78.44; H, 6.93; N, 7.22. Found: C, 78.24; H, 6.98; N, 7.21.

$L_b^{Q-2+} \cdot 2BPh_4^-$. Yield 65%. ¹H NMR (400 MHz, DMSO- d_6): δ 3.20 (s, 12H, CH₃), 3.63 (t, 8H, NCH₂), 3.77 (m, 8H, NCH₂CH₂), 6.77 (t, 8H, ArH), 6.91 (t, 16H, ArH), 7.16 (s, 16H, ArH), 8.00 (d, 4H, ArH), 0.807 (t, 2H, ArH), 9.33 (s, 4H, NH). FAB MS m/z 845 [M − BPh₄]⁺, 525 [M − H(BPh₄)₂]⁺. Anal. Calcd for C₇₄H₇₈B₂N₈O₄: C, 76.29; H, 6.75; N, 9.62. Found: C, 73.61; H, 6.55; N, 9.50.

Table 1. Crystallographic Data for $L_a^{Q_{2+}} \cdot 2Cl^- \cdot 2.66H_2O$ (1), $L_a^{Q_{2+}} \cdot H^+ \cdot 3HSO_4^- \cdot 3H_2O$ (2), $L_b^{Q_{2+}} \cdot 2I^- \cdot 2H_2O$ (3), and $L_c^{Q_{2+}} \cdot 2C_{24}H_{20}B^- \cdot 4CH_3OH$ (4)

	1	2	3	4
empirical formula	$C_{28}H_{45.33}Cl_2N_6O_{6.6}$	$C_{30}H_{50}N_6O_{19}S_3$	$C_{26}H_{42}I_2N_8O_6$	$C_{76}H_{92}B_2N_6O_8S_2$
formula weight	643.39	850.97	816.48	1303.30
crystal system	monoclinic	monoclinic	monoclinic	triclinic
space Group	$P2_1/n$	$P2_1/n$	$P2_1/c$	$P\bar{1}$
<i>a</i> (Å)	7.6011(6)	7.2836(2)	7.1904(4)	9.4804(6)
<i>b</i> (Å)	11.3704(9)	16.2898(4)	11.4396(6)	10.2714(6)
<i>c</i> (Å)	17.599(1)	35.9526(9)	20.2455(10)	19.8587(12)
α (deg)	90	90	90	104.080(2)
β (deg)	95.260(2)	91.434(2)°	90.681(2)°	92.140(2)
γ (deg)	90	90	90	112.731(2)
<i>V</i> (Å ³)	1514.7(2)	4264.38(19)	1665.18(15)	1711.25(18)
<i>Z</i>	2	4	2	1
<i>d</i> _{calc} (g/cm ³)	1.411	1.325	1.628	1.265
λ (Å)	0.71073	0.71073	0.71073	0.71073
<i>T</i> (K)	100(2)	100(2)	100(2)	100(2)
<i>F</i> (000)	685	1808	816	696
abs coeff (mm ⁻¹)	0.269	0.245	1.938	0.139
abs corr	semiempirical	semiempirical	semiempirical	semiempirical
max, min trans	0.995, 0.953	0.985, 0.875	0.893, 0.550	0.981, 0.963
θ range	2.14–30.01	1.69–25.00	2.04–30.50	2.14–26.00
reflns collected	12 395	22 278	13 813	10 889
indep reflns	4397	7238	4993	6372
<i>R</i> (int)	0.026	0.035	0.023	0.017
data/restr/param	4397/0/200	7965/7/557	4993/0/194	6372/0/424
$\langle R \rangle_1$; wR_2	0.046; 0.123	0.076; 0.199	0.028; 0.074	0.040; 0.109
GOF (<i>F</i> ²)	1.043	1.064	0.973	1.020
obsd data [<i>I</i> > 2σ(<i>I</i>)]	3527	5774	4736	5679
largest diff. peak and hole (e Å ⁻³)	0.49 and −0.27	1.24 and −0.71	2.06 and −0.44	0.37 and −0.27
$\langle R \rangle_1$ (obsd data) = $\Sigma F_o - F_c / \Sigma F_o $; wR_2 (all data) = $\{\Sigma [w(F_o^2 - F_c^2)^2] / \Sigma [w(F_o^2)]\}^{1/2}$.				

$L_c^{Q_{2+}} \cdot 2BPh_4^-$. Yield 75%. ¹H NMR (500 MHz, DMSO-*d*₆, TMS): δ 3.20 (s, 12H, CH₃), 3.56 (d, 8H, NCH₂), 3.99 (d, 8H, NCH₂), 6.77 (t, 8H, BArH), 6.92 (d, 16H, BArH), 7.17 (d, 16H, ArH), 7.46 (b, 4H, ArH), 8.81 (b, 4H, NH). FAB MS: *m/z* 1175.2 [*M* + 1]⁺. Anal. Calcd for C₂₄H₃₆N₆O₄S₂·B₂C₄₈H₄₀: C, 73.59; H, 6.47; N, 7.15. Found: C, 73.75; H, 6.53; N, 7.18.

$L_a^{Q_{2+}} \cdot 2X^-$. The HSO₄[−] and Cl[−] salts synthesized for crystallographic studies were obtained by adding a few drops of conc. H₂SO₄ or HCl to an aqueous solution of $L_a^{Q_{2+}} \cdot 2OH^-$ until a pH < 2 was reached. The respective salts were isolated as white solids after evaporation of the solvent. Because of the limited amount of sample, the isolated compounds were recrystallized without further analysis.

NMR Studies. ¹H NMR titrations of the ligands with *n*-Bu₄N⁺ salts of anions (A[−] = H₂PO₄[−], HSO₄[−], NO₃[−], Cl[−], Br[−], I[−], and ClO₄[−]) were carried out on a Bruker NMR spectrometer at 500 MHz. Both the ligands and anion salts were dissolved in DMSO-*d*₆. The initial concentration of the ligand was 2 mM. Aliquots of each anion from a stock solution (20 mM) were added directly to an NMR tube containing the ligand solution. Each titration was performed by 20 measurements at room temperature and repeated at least once to verify the results. All the proton signals were calibrated against trimethylsilane (TMS) used as an external reference in a sealed capillary tube. The association constants, *K*_a, were calculated by fitting the change in the several independent signals with a 1:1 association model from a nonlinear regression curve fitting program with Sigma Plot¹⁷ or EQNMR.¹⁸ The error limit in *K*_a was less than 10% based on the regression analysis of the experimental data.

X-ray Crystallography. Attempts to grow crystals of the quaternized salts with a variety of anions resulted in the isolation of the four different salts suitable for X-ray analysis.

$L_a^{Q_{2+}} \cdot 2Cl^- \cdot 2.66H_2O$ (1). Recrystallization of the Cl[−] salt from a CH₃OH solution afforded tiny prisms after 2 days under Et₂O diffusion.

$L_a^{Q_{2+}} \cdot H^+ \cdot 3HSO_4^- \cdot 3H_2O$ (2). Colorless plates were isolated from a CH₃OH/DMSO (3:1 v/v) solution of the sulfate salt after 2 wks under Et₂O diffusion.

$L_b^{Q_{2+}} \cdot 2I^- \cdot 2H_2O$ (3). Crystals were grown after 3 days by slow evaporation of an aqueous solution of the iodide salt at room temperature.

$L_c^{Q_{2+}} \cdot 2BPh_4^- \cdot 4(CH_3OH)$ (4). Crystals were isolated from the slow evaporation of a DMSO/MeOH solution of the tetraphenylborate salt at room temperature.

The crystallographic data and details of data collection for 1–4 are given in Table 1. Intensity data for all four crystals were collected using a Bruker SMART APEX CCD area detector mounted on a Bruker D8 goniometer using graphite-monochromated MoK_α radiation (λ = 0.71073 Å).¹⁹ The data were collected at 100(2) K, and intensity data were measured as a series of ω and θ oscillation frames. The detector was operated in 512 × 512 mode and was positioned 5.054 cm from the sample. Coverage of unique data to 2 θ (MoK_α) = 52.00° was 94.4–99.9% complete for all four structures. The data were corrected for absorption by the semiempirical method.²⁰ Lorentz and polarization corrections were applied, and the data were merged to form a set of independent data for each sample. Space groups were determined by systematic absences and statistical tests in the monoclinic samples 1, 2, and 3 and by statistical tests in the triclinic sample 4. The structures were solved by direct methods and refined by full-matrix least-squares methods on *F*².²¹ Non-hydrogen atoms were refined with anisotropic displacement parameters. Anticipated hydrogen atoms for all four structures were initially placed at idealized positions and refined isotropically at values of 1.2 (nonmethyl) or 1.5 (methyl) times the equivalent isotropic displacement parameter of the attached C, N, or O atom.

The structure of 2 was originally thought to contain a disordered DMSO solvent molecule of crystallization. However, when an unusually short (<2.5 Å) amide O...O separation was observed, indicating an

LBHB, it became evident that the disordered solvent was actually a HSO_4^- ion. When the additional HSO_4^- was included in the structural model, a small peak appeared in a difference Fourier midway between the two oxygen atoms involved in the short $\text{O}\cdots\text{O}$ separation. This electron density was included in the structural model of **2** as a hydrogen atom that was refined as an independent isotropic atom. The amide hydrogen atoms of **2** were also refined as independent isotropic atoms.

RESULTS AND DISCUSSION

Synthesis. The neutral tetraamides containing two tertiary amine centers L_{a-c} were readily synthesized using high dilution techniques, as reported earlier by us,^{5,6} and converted into quaternary salts by reacting with excess CH_3I under mild conditions.¹⁰ The compounds appeared as white solids after the reaction and were easily isolated as pure products. Preliminary NMR titrations of the I^- salts with other anions disappointingly did not show any significant change in the resonances, however, indicating that I^- was successfully competing with the added anion for binding. To minimize this competition effect, I^- was exchanged for the bulky BPh_4^- ion by passage through an ion exchange column containing OH^- followed by the addition of NaBPh_4 to yield $\text{L}_{a-c}^{\text{Q}^{2+}} \cdot 2\text{BPh}_4^-$. The eluted solution of $\text{L}_{a-c}^{\text{Q}^{2+}} \cdot 2\text{OH}^-$ from the ion exchange column was suitable to convert to salts of desired anions by reaction with inorganic acids.

Anion binding. The three macrocycles $\text{L}_{a-c}^{\text{Q}^{2+}}$ all contain four amide groups and two quaternized nitrogen centers. The two BPh_4^- bulky counteranions that serve to balance the charges were not expected to block the binding sites of the macrocycles. Support for this assumption was obtained crystallographically, by the absence of any observed hydrogen bonding interaction of BPh_4^- with the $\text{L}_{a-c}^{\text{Q}^{2+}}$ cation.

The binding properties of the ligands with a variety of inorganic anions were investigated by ^1H NMR titrations in $\text{DMSO}-d_6$. The addition of anions to $\text{L}_{a-c}^{\text{Q}^{2+}}$ resulted in typical downfield shifts of the ligand protons (Figure 1). The changes

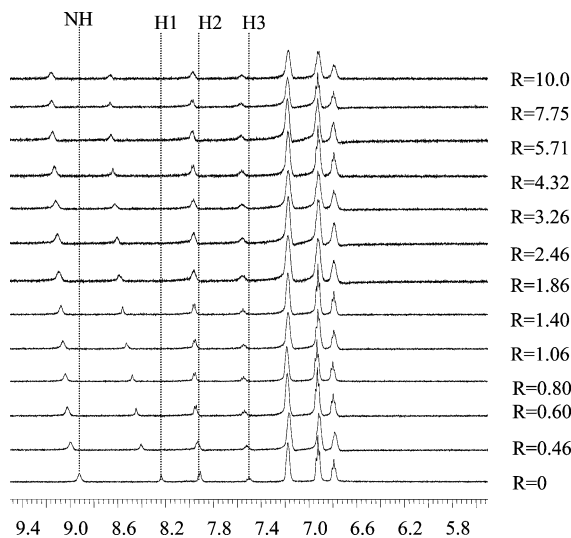


Figure 1. ^1H NMR spectra of the aromatic region of $\text{L}_{a-c}^{\text{Q}^{2+}}$ in $\text{DMSO}-d_6$ showing the change of amide and aromatic protons on the addition of varying amounts of $n\text{-Bu}_4\text{NCl}$ at 25°C . $R = [\text{Cl}^-]/[\text{L}_{a-c}^{\text{Q}^{2+}}]$; H1, H2, and H3 are three aromatic protons of the ligand.

in the chemical shifts of the ligands were plotted as a function of anion concentration, and the results for most anions gave satisfactory fits to a 1:1 (ligand/anion) association model, with the exception of H_2PO_4^- and HSO_4^- . A slow equilibrium was

observed in the case of $\text{L}_{b-c}^{\text{Q}^{2+}}$ with H_2PO_4^- , and the association constant was calculated from the intensities of the complexed and uncomplexed ligand signals. Although the addition of HSO_4^- to $\text{L}_{a-c}^{\text{Q}^{2+}}$ caused significant downfield shifts of the NMR signals, severe peak broadening of both aromatic and amide signals hampered fitting the data for calculation of the binding constant. The binding constants obtained were compared with those previously reported for the neutral L_a and L_b (Table 2).¹⁰

Table 2. Binding Constants K_a (in M^{-1}) of the Ligands with Anions in $\text{DMSO}-d_6$ at 25°C

anions	$\text{L}_{a-c}^{\text{Q}^{2+}}$	$\text{L}_{b-c}^{\text{Q}^{2+}}$	$\text{L}_{c-c}^{\text{Q}^{2+}}$	L_a	L_b	L_c
Cl^-	1700	56 230	130	25	490	20
Br^-	140	23 990	>10	20	515	<10
I^-	100	160	>10	<10	<10	<10
H_2PO_4^-	10 960	208 900 ^b	900	830	10 960	100
HSO_4^-	^a	7945	1500	795	107	<10
NO_3^-	45	210	<10	<10	<10	<10
ClO_4^-	40	250	<10	<10	<10	<10

^aCalculation complicated due to peak broadening of chemical shift after the addition of anion. ^bAt the upper limits for NMR determination.

As expected, the dipositively charged macrocycles $\text{L}_{a-c}^{\text{Q}^{2+}}$ and $\text{L}_{b-c}^{\text{Q}^{2+}}$ showed significantly higher binding for anions compared with the corresponding neutral amides, L_a and L_b (Table 2, Figure 2). Disappointingly, the ligand $\text{L}_{c-c}^{\text{Q}^{2+}}$ showed only a

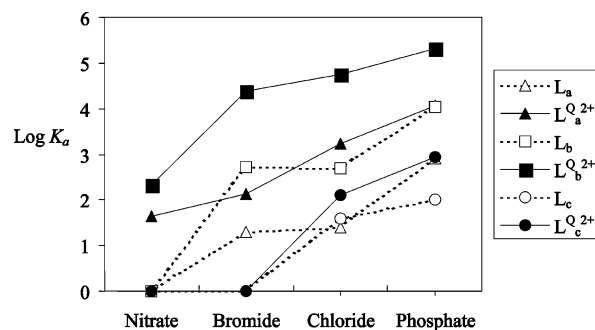


Figure 2. Binding profile of the quaternized amides, $\text{L}^{\text{Q}^{2+}}$ (solid lines), and neutral amides, L (dashed lines), for NO_3^- , Br^- , Cl^- , and H_2PO_4^- in $\text{DMSO}-d_6$ at 25°C .

moderate affinity for HSO_4^- and H_2PO_4^- and weak binding with Cl^- . For the other two quaternized ligands, however, the highest enhancement in affinity over the neutral analogue was found for Cl^- binding with the *m*-xylyl macrocycle $\text{L}_{a-c}^{\text{Q}^{2+}}$, with an enhancement factor of >60 over L_a . The other quaternized macrocycles exhibited a range of enhancement from approximately 6- to 10-fold.

As seen for the neutral L_a and L_b , $\text{L}_{a-c}^{\text{Q}^{2+}}$ and $\text{L}_{b-c}^{\text{Q}^{2+}}$ are highly selective for H_2PO_4^- . The selectivity observed for HSO_4^- by L_a was not seen in the quaternized $\text{L}^{\text{Q}^{2+}}$ s, however, which tends to support the supposition that the former (relative) high affinity derives from the Lewis base properties of the two amines. The receptor $\text{L}_{b-c}^{\text{Q}^{2+}}$ shows higher binding for all anions compared to $\text{L}_{a-c}^{\text{Q}^{2+}}$ as was generally found for the neutral corollaries L_b and L_c . This finding may in part be due to the influence of the pyridine nitrogen lone pair of electrons in preorganizing the macrocycle for binding by hydrogen bonding to the two adjacent amide hydrogen atoms, as discussed later in the crystal

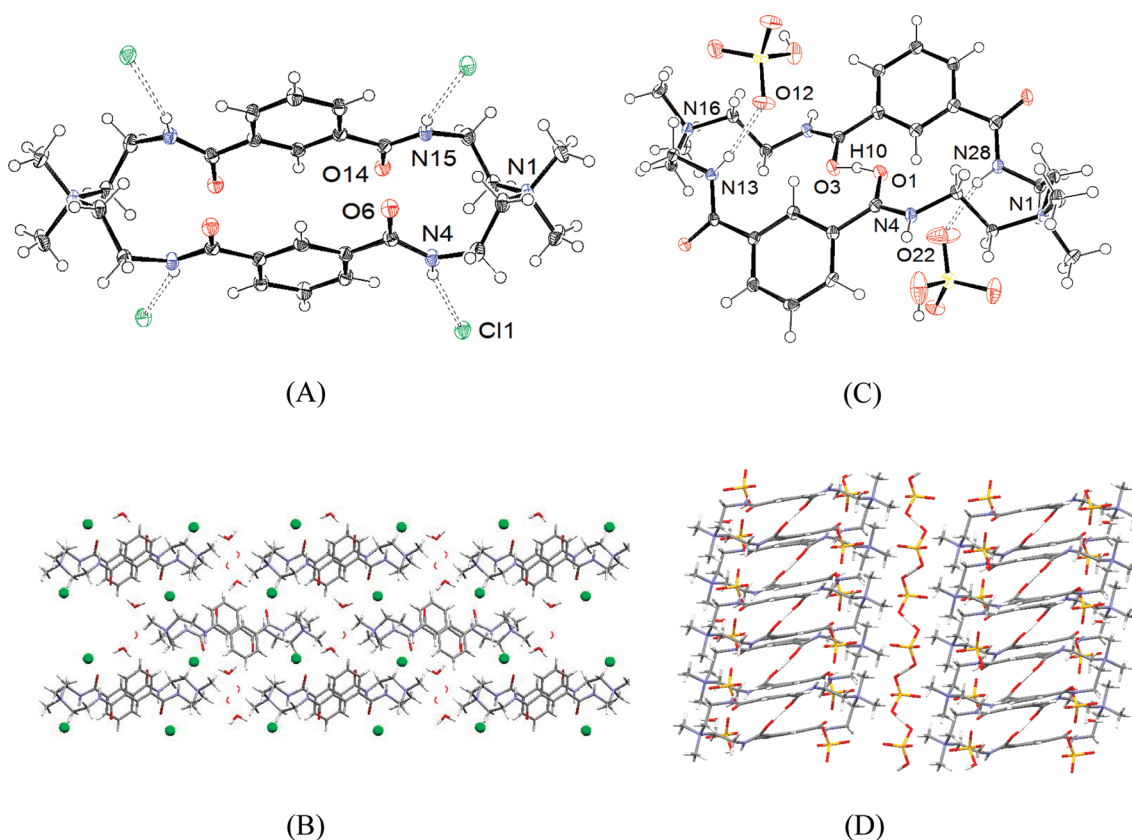


Figure 3. ORTEP views of the crystal structure (A) **1** and (C) **2** at 50% probability ellipsoids (water molecules are omitted for clarity); packing views (B) of **1** in the *bc* plane showing bridging Cl^- as viewed along the *a* axis and (D) of **2** viewed down the *b* axis.

structure of the iodide complex, **3**. The magnitude of binding for both $\text{L}_a^{\text{Q}^{2+}}$ and $\text{L}_b^{\text{Q}^{2+}}$ is especially noteworthy considering the high solvating capability of DMSO, which tends to lower affinities compared to nonpolar solvents. Overall, the expected enhancement of binding due to the added charge complementarity is seen for all anions for both $\text{L}_a^{\text{Q}^{2+}}$ and $\text{L}_b^{\text{Q}^{2+}}$. There generally do not appear to be any changes, however, in overall selectivity trends.

Crystal Structures. $\text{L}_a^{\text{Q}^{2+}} \cdot 2\text{Cl}^- \cdot 2.66\text{H}_2\text{O}$ (**1**). Single crystal X-ray diffraction studies of **1** indicate that the complex crystallizes with two Cl^- ions and 2.66 molecules of water per macrocycle. There are two formula units per unit cell, and the macrocycle sits on a crystallographic center of symmetry. The shape of the macrocyclic dication is elliptical, with the quaternized ammonium sites at opposite ends of the major axis of an approximate ellipsoid ($\text{N}(1) \cdots \text{N}(1)^* = 12.744 \text{ \AA}$) (Figure 3A). The stretched cavity serves to minimize the electrostatic repulsion between these two groups. The elongated structure also appears to be stabilized by the stacking of the two *m*-xylyl rings at a relatively short distance of $3.196(8) \text{ \AA}$. The amides are oriented with the carbonyl groups directed inside the cavity, while the amide protons that point outside the cavity are hydrogen bonded with symmetry-related Cl^- ions ($\text{N}(4) \cdots \text{Cl}(1) = 3.227(2) \text{ \AA}$ and $\text{N}(15) \cdots \text{Cl}(1)^* = 3.258(2) \text{ \AA}$) (Table 3). Hydrogen bonding interactions also occur between an external water molecule and both a Cl^- ion and O(14) of the receptor. The hydrogen bond motif is relayed throughout the structure, with chlorides and waters serving as links between the cationic macrocycles (Figure 3B).

$\text{L}_a^{\text{Q}^{2+}} \cdot \text{H}^+ \cdot 3\text{HSO}_4^- \cdot 3\text{H}_2\text{O}$ (**2**). The unusual encircled proton complex, $\text{L}_a^{\text{Q}^{2+}} \cdot \text{H}^+ \cdot 3\text{HSO}_4^- \cdot 3\text{H}_2\text{O}$ (**2**), crystallized in the

Table 3. Selected hydrogen bonding interactions of the anions and solvent molecules in $\text{L}_a^{\text{Q}^{2+}} \cdot 2\text{Cl}^- \cdot 2.66\text{H}_2\text{O}$ (**1**), $\text{L}_a^{\text{Q}^{2+}} \cdot \text{H}^+ \cdot 3\text{HSO}_4^- \cdot 3\text{H}_2\text{O}$ (**2**), $\text{L}_b^{\text{Q}^{2+}} \cdot 2\text{I}^- \cdot 2\text{H}_2\text{O}$ (**3**), $\text{L}_c^{\text{Q}^{2+}} \cdot 2\text{C}_{24}\text{H}_{20}\text{B}^- \cdot 4\text{CH}_3\text{OH}$ (**4**)

atoms	distances (Å)	atoms	distances (Å)
1			
$\text{N}(4) - \text{H}(4) \cdots \text{Cl}(1)$	3.227(1)	$\text{O}(1\text{S}) - \text{H}(1\text{SB}) \cdots \text{O}(14)$	2.790(2)
$\text{N}(15) - \text{H}(15) \cdots \text{Cl}(1)^a$	3.258(1)	$\text{O}(2\text{S}) - \text{H}(2\text{SA}) \cdots \text{O}(1\text{S})$	2.620(4)
$\text{O}(1\text{S}) - \text{H}(1\text{SA}) \cdots \text{Cl}(1)^b$	3.249 (1)	$\text{O}(2\text{S}) - \text{H}(2\text{SB}) \cdots \text{O}(1\text{S})^c$	2.631(4)
2			
$\text{N}(4) - \text{H}(4) \cdots \text{O}(23)$	2.869(4)	$\text{N}(28) - \text{H}(28) \cdots \text{O}(22)$	2.847(5)
$\text{N}(13) - \text{H}(13) \cdots \text{O}(12)$	2.834(4)	$\text{O}(1) - \text{H}(10) \cdots \text{O}(3)$	2.453(3)
$\text{N}(19) - \text{H}(19) \cdots \text{O}(14)$	2.859(4)		
3			
$\text{N}(4) - \text{H}(4) \cdots \text{I}(1)$	3.667 (2)	$\text{O}(1\text{S}) - \text{H}(1\text{SA}) \cdots \text{O}(14)$	2.804(2)
$\text{N}(15) - \text{H}(15) \cdots \text{I}(1)$	3.694 (2)	$\text{O}(1\text{S}) - \text{H}(1\text{SB}) \cdots \text{I}(2)$	3.576(2)
4			
$\text{N}(12) - \text{H}(12) \cdots \text{O}(1\text{T})$	2.978(2)	$\text{O}(1\text{T}) - \text{H}(1\text{T}) \cdots \text{O}(1\text{S})^d$	2.734(2)
$\text{O}(1\text{S}) - \text{H}(1\text{S}) \cdots \text{O}(18)$	2.795 (2)		

^aSymmetry transformations used to generate equivalent atoms: $x + 1/2, -y + 1/2, z + 1/2$. ^b $-x + 3/2, y + 1/2, -z + 1/2$. ^c $-x + 2, -y + 2, -z + 1$. ^d $x + 1, y, z$.

monoclinic space group $P2_1/n$. Included in the structure are the dicationic host and two nearby HSO_4^- anions, satisfying the charge on the macrocycle. However, what was not anticipated in the structure was the close approach of the two macrocyclic amide carbonyl groups ($\text{O} \cdots \text{O} = 2.453 \text{ \AA}$), which led to the discovery of a proton bound midway between the two oxygen

atoms (Figure 3C). The proximity of the two oxygen atoms apparently forces the phenyl groups to be offset from each other, contrary to the rather symmetrical placement of the phenyl groups in the Cl^- structure (Figure 3A). Likewise, the two quaternized groups are slightly closer to each other at 12.13 Å compared with the 12.74 Å observed in the Cl^- complex.

What is of most interest, however, is the very short *intramolecular* O1...O3 distance of 2.453(3) Å, which, along with the O...H...O angle of 173(5)° and O...H distances averaging 1.23(6) Å, are indicative of a symmetrical, low-barrier hydrogen bond (LBHB).¹⁶ It has been proposed that very short hydrogen bonds such as these are important in a variety of biological processes, such as in the stabilization of transition states.^{14,22–24}

Energy-wise, hydrogen bonds in the normal ranges, such as 2.8 Å and above for those between oxygen atoms, have a double-well potential. In these cases, the hydrogen atom is associated more strongly with one of the heteroatoms rather than equally with both. The barrier for exchange between the heteroatoms decreases with distance down to about 2.55 Å, where a zero point energy is reached, and the hydrogen can freely move between the two heteroatoms. At this point, the hydrogen bond is defined as a LBHB. At shorter distances, down to about 2.29 Å, where a single well potential exists, the hydrogen bond is dubbed as a short-strong hydrogen bond (SSHB).¹⁴

The O...O distance observed in the quaternized macrocycle is very similar to those reported for *intermolecular* hydrogen bonds in hemiprotonated amide oxygen atoms¹³ and somewhat shorter than the *intramolecular* distance in benzoylacetone (2.502 Å).¹⁴ As might be anticipated, the presence of the hydrogen bond also affects, albeit to a small extent, the bond order of the C=O and C–N linkages, compared to the other two amides. The bond lengths are N–C = 1.319(5) Å and C–O = 1.272(4) Å for the amide bonds associated with the LBHB compared to 1.346(5) and 1.240(4) Å for the N–C and C–O distances for the other two amides. These distances indicate a slightly diminished double bond character for the carbonyl C=O bond and increased double bond character for the N–C bond.

Outside of the macrocyclic circle, three HSO_4^- ions and three water molecules (one of which is only partial occupancy) comprise the rest of the crystal lattice. As with the Cl^- structure, two HSO_4^- ions lie directly outside of the macrocycle and are linked via hydrogen bonds to the two amide nitrogen atoms within an independent unit. These HSO_4^- ions also bridge to a neighboring macrocycle, so the structure is somewhat similar to that shown in Figure 3A for the Cl^- structure, although only two of the surrounding HSO_4^- ions are shown for clarity in Figure 3C. Hydrogen bond distances range from about 2.83–2.87 Å (Table 3). The three water molecules are hydrogen bonded with the HSO_4^- ions but not the macrocycle. What was originally thought to be a disordered DMSO molecule actually turned out, after recognizing the short O...O separation and LBHB, to be the third HSO_4^- . While slightly disordered, the HSO_4^- links to other HSO_4^- ions via a chain that forms a helical pattern down the *a* axis (Figure 3D). Although it would be of interest to know if the LBHB structure exists in solution, NMR evidence is ambiguous. While a very broad signal at 12.11 ppm was observed during a titration of the ligand with H_2SO_4 , LBHB resonances usually occur at slightly lower fields at around 15 ppm.²⁵

$\text{L}^{\text{Q}_b^{2+}} \cdot 2\text{I}^- \cdot 2\text{H}_2\text{O}$ (3). In 3 there are two asymmetric units, with each containing one-half of the cation, an iodide on a crystallographic mirror (I(1)) and another iodide on a center of symmetry (I(2)). A water molecule of crystallization sits on a general position. The pyridine macrocycle $\text{L}^{\text{Q}_b^{2+}}$ is conformationally quite different from that observed in either of the two crystal structures of $\text{L}^{\text{Q}_a^{2+}}$ (Figure 4A). $\text{L}^{\text{Q}_b^{2+}}$ is folded with the aromatic groups parallel to each other and separated by 3.547(8) Å. The amide hydrogen atoms point toward the pyridine nitrogen atoms (*syn–syn*), which is assumed to be facilitated by interactions between the pyridine lone pair of electrons, as also observed by others.^{26–29} This conformational change allows the macrocycle to fold and brings the quaternized amines much closer to each other ($\text{N}(1) \cdots \text{N}(1)^* = 6.527(2)$ Å). There are two symmetry independent iodides in the structure. One is held in a chelate-like hydrogen bonding interaction with the macrocyclic amides ($\text{N}(4) \cdots \text{I}(1) = 3.667(2)$ Å and $\text{N}(15) \cdots \text{I}(1) = 3.694(2)$ Å). The other symmetry unrelated

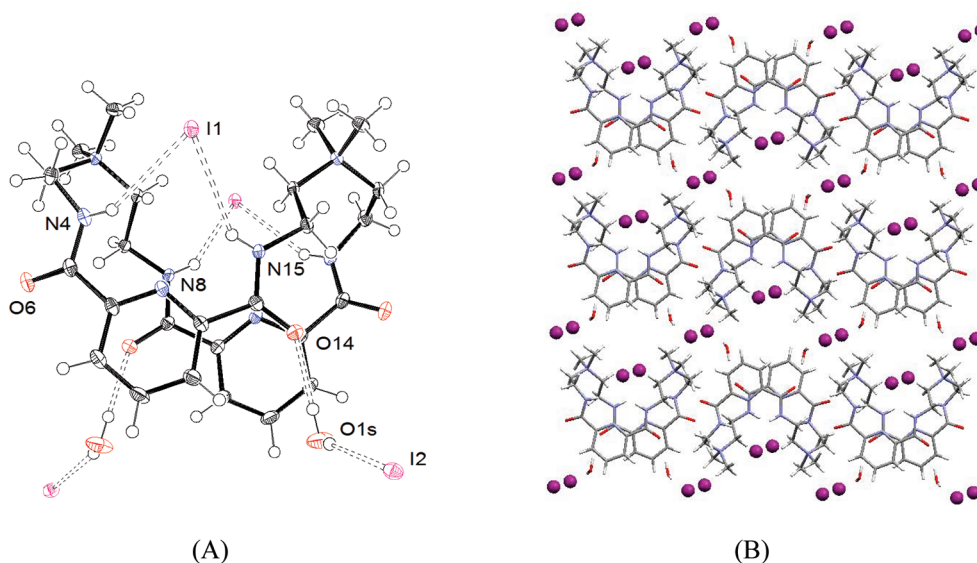


Figure 4. (A) ORTEP view of the crystal structure 3 at 50% probability ellipsoids and (B) packing view of the *bc* plane as viewed along the *a* axis. The two independent iodide ions are labeled, and the other two shown are symmetry related.

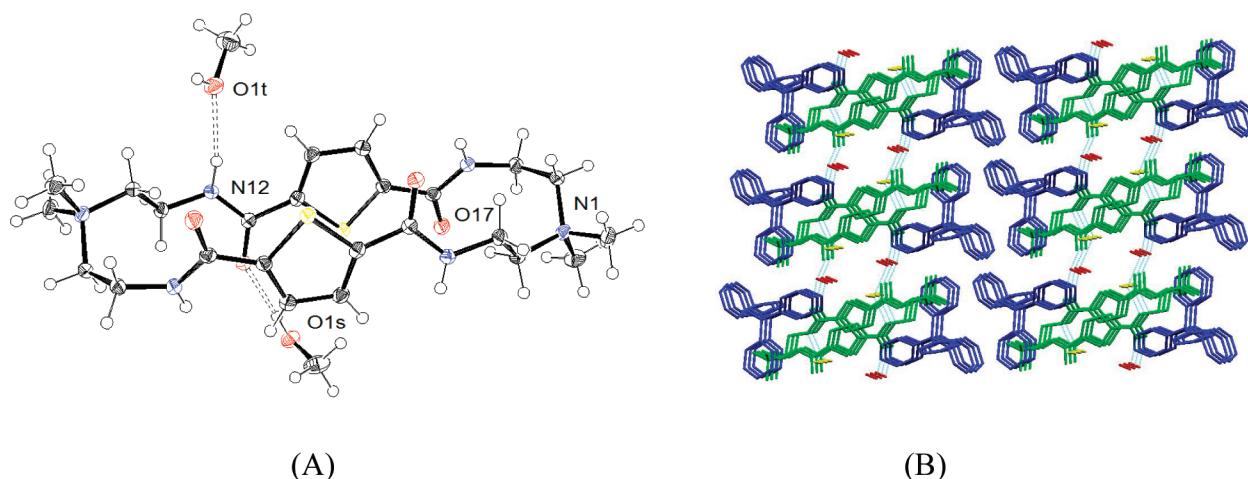


Figure 5. (A) ORTEP view of the crystal structure **4** at 50% probability ellipsoids and (B) packing view of *bc* plane as viewed along the *a* axis.

iodide ($I(2)$) is hydrogen bonded only with a water molecule. As seen in the packing view (Figure 4B), adjacent macrocycles fold in opposite directions forming a columnar-like structure, and the anions and the solvent molecules are held between adjacent layers. In addition to the preorganization of the amide hydrogen atoms as noted above, it is proposed that the opportunity for chelate-like binding by proximal hydrogen atoms also plays a role in the increased anion affinity seen for L_b and $L_b^{Q^{2+}}$ compared to L_a and $L_a^{Q^{2+}}$.

$L_c^{Q^{2+}} \cdot 2BPh_4^- \cdot 4(CH_3OH)$ (**4**). In the quaternized thiophene macrocycle, the complex crystallizes with two Ph_4B^- counterions and four CH_3OH molecules of crystallization, and the macrocycle sits on a center of symmetry. The conformation of the macrocycle is similar to that seen for **1**, with a distance of 12.984 Å between the two quaternized nitrogen centers (Figure 5A). The macrocycle is essentially free from any interaction with the bulky anion groups, which are located at the two ends of the macrocycle, near the quaternized nitrogen centers. The two thiophene groups are oriented in *anti* conformations and are stacked at a distance of 3.64 Å from each other. All four CH_3OH molecules are involved in hydrogen bonding with either amidic protons or carbonyl oxygen atoms. Two symmetry-related CH_3OH oxygen atoms (O(1T)) are hydrogen bonded with amide protons of N(12) ($N-H \cdots O = 2.978(2)$ Å), and the hydroxyl hydrogen atoms of the remaining two symmetry-related CH_3OH s (H(1T)) are hydrogen bonded with the carbonyl oxygen atoms of O(18) ($O-H \cdots O = 2.795(2)$ Å). The oxygen of a symmetry-related O(1S) is also hydrogen bonded with the hydroxyl hydrogen of O(1T). The extended packing diagram (Figure 5B) shows the layer-like packing of the macrocycles, separated by the bulky $2BPh_4^-$ groups.

SUMMARY

Three trends are seen: the increased magnitude of anion affinity of $L_{a-c}^{Q^{2+}}$ compared to L_{a-c} , the increased binding observed in general for the pyridine (**b**) compared to the *m*-xylyl (**a**) analogues, and the diminished binding seen for the thiophene spacer. The increased binding observed for the quaternized $L^{Q^{2+}}$ compared to **L** can be traced to the addition of charge complementarity, i.e., the result of added electrostatic attraction. The enhanced binding observed for $L_b^{Q^{2+}}$ can most probably be attributed to the pyridine-assisted preorganization of the amide protons. The result is an increased propensity for chelate-like binding to hold the anion more firmly

in place, compared to the unidentate coordination seen for **1** and **2**. While thiophene, like *m*-xylyl and pyridine, possesses considerable aromatic character by virtue of its two four carbon π electrons and the two lone pairs on the sulfur, it is highly unreactive at the sulfur site. For example, it does not tend to form salts, unlike pyridine (e.g., pyridinium salts).³⁰ Thus, it would not be expected to exhibit the hydrogen bonding tendencies observed for the pyridine nitrogen, and the diminished binding observed for the thiophene may merely be due to the electronic role that the two lone pairs of the sulfur play in modulating the Lewis base strength of the amide hydrogen atoms.

The unanticipated bonus of the study was the isolation and characterization of the HSO_4^- complex with the LBHB. Such a finding provides support for similar short contacts that might be occurring in the complex interior cavities of proteins. If confirmed, such interactions may indeed play a significant role in protein structure and function. Further studies are currently underway to understand what must be a delicate interplay of the acid/base subtleties leading to this unusual occurrence.

In conclusion, the quaternized macrocycles show stronger binding for anions compared to their neutral precursors, and both the neutral and quaternized pyridine macrocycles show higher binding than the *m*-xylyl derivatives. The enhanced binding and structural insight on these anion receptors demonstrate the significance of adding electrostatic complementarity and/or in promoting preorganization and chelation effects to a neutral anion receptor.

ASSOCIATED CONTENT

Supporting Information

Crystallographic data for **1–4** in CIF formats. This material is available free of charge via the Internet at <http://pubs.acs.org>.

AUTHOR INFORMATION

Corresponding Author

*E-mail: kbjames@ku.edu.

Notes

The authors declare no competing financial interest.

ACKNOWLEDGMENTS

We thank the National Science Foundation CHE-0854967 for support of this work and for a CAREER award (CHE-1056927) to M.A.H. The assistance of Dr. Douglas Powell, currently at

the Department of Chemistry and Biochemistry, University of Oklahoma, and the X-ray Crystallography Laboratory at the University of Kansas are acknowledged for providing the crystal structure data.

REFERENCES

- (1) (a) Bianchi, A.; Bowman-James, K.; García-España, E., Eds. *Supramolecular Chemistry of Anions*; Wiley-VCH: New York, 1997. (b) Stibor, I., Ed. *Anion Sensing*; Springer: Berlin, Germany, 2005. (c) Sessler, J. L.; Gale, P. A.; Cho, W.-S. *Anion Receptor Chemistry*; RSC Publishing: Cambridge, U.K., 2006. Bowman-James, K.; Bianchi, A.; García-España, E., Eds.; *Anion Coordination Chemistry*; Wiley-VCH: Berlin, Germany, 2012.
- (2) Themed issues: (a) Lever, A. B. P.; Gale, P. A., Eds. 35 Years of Synthetic Anion Receptor Chemistry, 1968–2003. *Coord. Chem. Rev.* **2003**, *240* (1–2), 1–226. (b) Lever, A. B. P.; Gale, P. A., Eds. *Coord. Chem. Rev.* **2006**, *250*, 2917–3244. (c) Gale, P. A.; Gunnlaugsson, T., Eds. *Supramolecular Chemistry of Anionic Species*. *Chem. Soc. Rev.* **2010**, *39* (10), 3581–4008.
- (3) Selected recent reviews: (a) Kubik, S.; Reyheller, C.; Stüwe, S. *J. Inclusion Phenom. Macrocyclic Chem.* **2005**, *52*, 137–187. (b) Kang, S. O.; Begum, R. A.; Bowman-James, K. *Angew. Chem., Int. Ed.* **2006**, *45*, 7882–7894. (c) Kang, S. O.; Hossain, M. A.; Bowman-James, K. *Coord. Chem. Rev.* **2006**, *250*, 3038–3052. (d) Gale, P. A. *Acc. Chem. Res.* **2006**, *39*, 465–475. (e) Schmidtchen, F. P. *Coord. Chem. Rev.* **2006**, *250*, 2918–2928. (f) Lankshear, M. D.; Beer, P. D. *Acc. Chem. Res.* **2007**, *40*, 657–668. (g) Gale, P. A. *Chem. Commun.* **2008**, 4525–4540. (h) Gale, P. A.; García-Garrido, S. E.; Garric, J. *Chem. Soc. Rev.* **2008**, *37*, 151–190. (m) Caltagirone, C.; Gale, P. A. *Chem. Soc. Rev.* **2009**, *38*, 520–563. (n) Wenzel, M.; Hiscock, J. R.; Gale, P. A. *Chem. Soc. Rev.* **2012**, *41*, 480–520.
- (4) (a) Luecke, H.; Quirocho, F. A. *Nature* **1990**, *347*, 402–406. (b) He, J. J.; Quirocho, F. A. *Science* **1991**, *251*, 1479–1483.
- (5) Hossain, M. A.; Llinares, J. M.; Powell, D.; Bowman-James, K. *Inorg. Chem.* **2001**, *40*, 2936–2937.
- (6) Hossain, M. A.; Kang, S. O.; Llinares, J. M.; Powell, D.; Bowman-James, K. *Inorg. Chem.* **2003**, *42*, 5043–5045.
- (7) (a) Danby, A.; Seib, L.; Alcock, N. W.; Bowman-James, K. *Chem. Commun.* **2000**, 973–974. (b) Kang, S. O.; Llinares, J. M.; Powell, D.; VanderVelde, D.; Bowman-James, K. *J. Am. Chem. Soc.* **2003**, *125*, 10152–10153. (c) Kang, S. O.; VanderVelde, D.; Powell, D.; Bowman-James, K. *J. Am. Chem. Soc.* **2004**, *126*, 12272–12273. (d) Kang, S. O.; Hossain, M. A.; Powell, D.; Bowman-James, K. *Chem. Commun.* **2005**, 320–330. (e) Kang, S. O.; Powell, D.; Bowman-James, K. *J. Am. Chem. Soc.* **2005**, *127*, 13478–13479. (f) Kang, S. O.; Powell, D.; Bowman-James, K. *Angew. Chem.* **2006**, *45* (12), 1921–1925. (g) Kang, S. O.; Powell, D.; Day, V. W.; Bowman-James, K. *Cryst. Growth Des.* **2007**, *7*, 606–608. (h) Kang, S. O.; Day, V. W.; Bowman-James, K. *Org. Lett.* **2008**, *10*, 2677–2680. (i) Kang, S. O.; Day, V. W.; Bowman-James, K. *Org. Lett.* **2009**, *11*, 3654–3657. (j) Kang, S. O.; Day, V. W.; Bowman-James, K. *J. Org. Chem.* **2010**, *75* (2), 277–283. (k) Kang, S. O.; Day, V. W.; Bowman-James, K. *Inorg. Chem.* **2010**, *49*, 8629–8636. (l) Wang, Q.-Q.; Day, V. W.; Bowman-James, K. *Chem. Sci.* **2011**, *2*, 1735–1738. (m) Wang, Q.-Q.; Day, V. W.; Bowman-James, K. *Angew. Chem., Int. Ed.* **2012**, *51*, 2119–2123.
- (8) (a) Kavallieratos, K.; Danby, A.; Van Berkel, G. J.; Kelly, M. A.; Sachleben, R. A.; Moyer, B. A.; Bowman-James, K. *Anal. Chem.* **2000**, *72*, 5258–5264. (b) Qian, Q.; Wilson, G. S.; Bowman-James, K.; Girault, H. H. *Anal. Chem.* **2001**, *73*, 497–503. (c) Fowler, C. J.; Haverlock, T. J.; Moyer, B. A.; Shriver, J. A.; Gross, D. E.; Marquez, M.; Sessler, J. L.; Hossain, M. A. *J. Am. Chem. Soc.* **2008**, *130*, 14386–14387. (d) Moyer, B. A.; Sloop, F. V. Jr.; Fowler, C. J.; Haverlock, T. J.; Kanga, H.-A.; Delmau, L. H.; Bau, D. M.; Hossain, M. A.; Bowman-James, K.; Shriver, J. A.; Bill, N. L.; Gross, D. E.; Marquez, M.; Lynch, V. M.; Sessler, J. L. *Supramol. Chem.* **2010**, *22*, 653–671.
- (9) Day, V. W.; Hossain, M. A.; Kang, S. O.; Powell, D.; Lushington, G.; Bowman-James, K. *J. Am. Chem. Soc.* **2007**, *129*, 8692–8693.
- (10) Hossain, M. A.; Kang, S. O.; Powell, D.; Bowman-James, K. *Inorg. Chem.* **2003**, *42*, 1397–1399.
- (11) Wisner, J. A.; Beer, P. D.; Drew, M. G. B. *Angew. Chem., Int. Ed.* **2001**, *40*, 3606–3609.
- (12) Kral, V.; Rusin, O.; Schmidtchen, F. P. *Org. Lett.* **2001**, *3*, 873–876.
- (13) (a) Miyahara, Y.; Tanaka, Y.; Amimoto, K.; Akazawa, T.; Sakuragi, T.; Kobayashi, H.; Kubota, K.; Suenaga, M.; Koyama, H.; Inazu, T. *Angew. Chem., Int. Ed.* **1999**, *38*, 956–959. (b) Winkler, F. K.; Dunitz, J. D. *Acta Crystallogr., Sect. B: Struct. Crystallogr. Cryst. Chem.* **1975**, *31*, 283–286. (c) Winkler, F. K.; Dunitz, J. D. *Acta Crystallogr., Sect. B: Struct. Crystallogr. Cryst. Chem.* **1975**, *31*, 286–288. (d) Levshin, I. B.; Kaganskii, M. M.; Vyunov, K. A.; Tsurkan, A. A.; Ginak, A. I.; Espenbetov, A. A.; Yanovsky, A. I.; Struchkov, Y. T. *Zh. Prikl. Spektrosk.* **1982**, *37*, 103–107. (e) Herstein, F. H.; Kapon, M.; Schwotzer, W. *Helv. Chim. Acta* **1983**, *66*, 35–43. (f) Jaber, M.; Guilhem, J.; Loiseleur, H. *Acta Crystallogr., Sect. C: Cryst. Struct. Commun.* **1983**, *39*, 485–487. (g) Kildea, J. D.; White, A. H. *Inorg. Chem.* **1984**, *23*, 3825–3827. (h) Boeyens, J. C.; Denner, A. L.; Howard, A. S.; Michael, J. P. S. *Afr. J. Chem.* **1986**, *39*, 217–220. (i) Avenoz, A.; Busto, J. H.; Cativiela, C.; Peregrine, J. M.; Rodríguez, F. *Tetrahedron* **1998**, *54*, 11659–11674. (j) Escudero, E.; Subirana, J. A.; Solans, X. *Acta Crystallogr., Sect. C: Struct. Cryst. Commun.* **1999**, *55*, 644–646. (k) Wilhelm, M.; Koch, R.; Strasdeit, H. *New J. Chem.* **2002**, *26*, 560–566. (l) Bekaert, A.; Lemoine, P.; Biossat, B.; Jouan, M.; Gemeiner, P.; Brion, J. D. *J. Mol. Struct.* **2005**, *738*, 39–44.
- (14) Schiøtt, B.; Iversen, B. B.; Madsen, G. K. H.; Larsen, F. K.; Bruice, T. C. *Proc. Natl. Acad. Sci. U.S.A.* **1998**, *95*, 12799–12802.
- (15) (a) Gubin, A. I.; Yanovsky, A. I.; Struchkov, Y. T.; Nurakhmetov, N. N.; Buranbaev, M. Z.; Beremzhanov, B. A. *Izv. Akad. Nauk. Kaz. SSR, Ser. Khim.* **1986**, *78*–81. (b) Gubin, A. I.; Buranbaev, M. Z.; Erkasov, R. S.; Nurakhmetov, N. N.; Khakimzhanova, G. D. *Kristallografiya* **1989**, *34*, 1305.
- (16) Hibbert, F.; Emsley, J. *Adv. Phys. Org. Chem.* **1990**, *26*, 255–279.
- (17) Schneider, H.-J.; Kramer, R.; Simova, S.; Schneider, U. *J. Am. Chem. Soc.* **1988**, *110*, 6442–6448.
- (18) Hynes, M. J. *J. Chem. Soc., Dalton Trans.* **1993**, 311–312.
- (19) Data collection: SMART Software Reference Manual; Bruker-AXS: Madison, WI, 1994. Data reduction: SAINT Software Reference Manual; Bruker-AXS, Madison, WI, 1995.
- (20) Sheldrick, G. M. *SADABS, Program for Empirical Absorption Correction of Area Detector Data*; University of Göttingen: Germany, 1996.
- (21) Sheldrick, G. M. *SHELXTL Version 5 Reference Manual*; Bruker AXS: Madison, WI, 1994. *International Tables for Crystallography*, Vol. C; Kluwer: Boston, MA, 1995; Tables 6.1.1.4, 4.2.6.8, and 4.2.4.2.
- (22) Ash, E. L.; Sudmeier, J. L.; De Fabo, E. C.; Bachovchin, W. W. *Science* **1997**, *278*, 1128–1132.
- (23) Perrin, C. L.; Nielson, J. B. *Annu. Rev. Phys. Chem.* **1997**, *48*, 511–544.
- (24) Cleland, W. W.; Frey, P. A.; Gerlt, J. A. *J. Biol. Chem.* **1998**, *273*, 25529–25532.
- (25) Springborg, J.; Olsen, C. E.; Sotofte, I. *Acta Chem. Scand.* **1995**, *49*, 555–563.
- (26) Huang, B.; Parquette, J. R. *Org. Lett.* **2000**, *2*, 239–242.
- (27) (a) Szumna, A.; Gryko, D. T.; Jurczak, J. *Heterocycles* **2002**, *56*, 361–368. (b) Chmielewski, M. J.; Zieliński, T.; Jurczak, J. *Pure Appl. Chem.* **2007**, *79*, 1087–1096.
- (28) Baer, A. J.; Koivisto, B. D.; Côté, A. P.; Taylor, N. J.; Hanan, G. S.; Nierengarten, H.; Van Dorsselaer, A. *Inorg. Chem.* **2002**, *41*, 4987–4989.
- (29) Ghosh, S.; Roehm, B.; Begum, R. A.; Kut, J.; Hossain, M. A.; Day, V. W.; Bowman-James, K. *Inorg. Chem.* **2007**, *46*, 9519–9521.
- (30) Roberts, J. D.; Caserio, M. C. *Basic Principles of Organic Chemistry*; W. A. Benjamin, Inc.: New York, 1965; pp 979–983.